Fabrication of a novel antifouling TiO2/CPTES/metformin-PES nanocomposite membrane for removal of various organic pollutants and heavy metal ions from wastewater

Article · May 2020

DOI: 10.1007/s11696-020-01178-2

4 authors, including:

Vahid Barahimi
Isfahan University of Technology

Ramezan Ali Taheri
Baqiyatallah University of Medical Sciences

Amirhossein Mazaheri
University of Tehran

Fabrication of a novel antifouling TiO_2/CPTES/metformin-PES nanocomposite membrane for removal of various organic pollutants and heavy metal ions from wastewater

Vahid Barahimi, Ramezan Ali Taheri, Amirhossein Mazaheri & Hamid Moghimi

Chemical Papers

ISSN 2585-7290
Volume 74
Number 10

Chem. Pap. (2020) 74:3545-3556
DOI 10.1007/s11696-020-01178-2

Springer

Chemical Papers (2020) 74:3545–3556
https://doi.org/10.1007/s11696-020-01178-2

ORIGINAL PAPER

Fabrication of a novel antifouling TiO_2/CPTES/metformin-PES nanocomposite membrane for removal of various organic pollutants and heavy metal ions from wastewater

Vahid Barahimi[1] · Ramezan Ali Taheri[1] · Amirhossein Mazaheri[2] · Hamid Moghimi[3]

Received: 10 December 2019 / Accepted: 28 April 2020 / Published online: 14 May 2020

Abstract

The present study focuses on the synthesis of high-antifouling TiO_2/3-cyanopropyltriethoxysilane (CPTES)/Metformin-polyethersulfone (PES) membrane with various dosages of NPs (0.1, 0.5 and 1 wt%). The performance of the membranes was studied by the rejection of Cu(II) ions, COD content and dye removal from liquorice extraction plant (LEP) wastewater. The properties of the prepared nanoparticles (NPs) and membranes were identified by XRD, SEM, FT-IR, contact angle and AFM analyses. The permeability and antifouling tests were performed for all the blended nanocomposite membranes. The addition of NPs in the membrane network improves membrane hydrophilicity, permeate flux and flux recovery ratio (FRR) values due to the presence of amine, hydroxyl and silica groups on the membrane surface. The M_4 (1 wt% of NPs) membrane is selected as an optimal nanocomposite membrane which exhibits a much higher pure water flux (37.2 kg m^{-2} h^{-1}) and FRR value (98%). Also, the high permeation flux (25 kg m^{-2} h^{-1}), COD removal (88%) and dye removal (98%) were achieved during filtration of LEP wastewater with COD concentration of 800 mg l^{-1} at pressure of 5 bar after 150 min.

Keywords PES nanofiltration membrane · TiO_2/CPTES/metformin nanoparticles · Antifouling · Direct red 16 as an azo dye · Liquorice extraction plant wastewater · Heavy metal

List of symbols

CPTES	Cyanopropyltriethoxysilane
TBOT	Tetran-butylorthotitanate
TEOS	Tetraethyl orthosilicate
SEM	Scanning electron microscopy
AFM	Atomic force analysis
FRR	Flux recovery ratio
PES	Polyethersulfone
NF	Nanofiltration
MWCNTs	Multiwalled carbon nanotubes
B-TiO_2–SiO_2/$CoFe_2O_4$	Boron doped-TiO_2–SiO_2 cobalt ferrite
XRD	X-ray diffraction
FT-IR	Fourier transform infrared
NPs	Nanoparticles
PVP	Polyvinylpyrrolidone
PWF	Pure water flux
C_f	Particular concentration in feed
C_p	Particular concentration in permeate
DMAc	*N*,*N*-dimethylacetamide
J_p	Powder milk solution flux
$J_{w,1}$	Pure water flux
$J_{w,2}$	Pure water flux after fouling
R_t	Total fouling resistance
R_r	Reversible fouling resistance
R_{ir}	Irreversible fouling resistance
M_1	Unfilled PES membrane
M_2	Membrane with 0.1 wt% nanoparticle
M_3	Membrane with 0.5 wt% nanoparticle
M_4	Membrane with 1 wt% nanoparticle
COD	Chemical oxygen demand

✉ Ramezan Ali Taheri
taheri@bmsu.ac.ir

1 Nanobiotechnology Research Center, Baqiyatallah University of Medical Sciences, Tehran, Iran

2 Department of Mechanical Engineering, Isfahan University of Technology, Isfahan, Iran

3 Department of Microbial Biotechnology, School of Biology, College of Science, University of Tehran, Tehran, Iran

Introduction

Liquorice wastewater is a thick and brownish slurry waste that has water-soluble components with an unpleasant odor. It is a major source of pollution if it is discharged untreated into receiving waters, causing considerable environmental problems. The chemical oxygen demand (COD) content of liquorice wastewater is too high. Also, it is characterized as a low biodegradable wastewater. The effluent with low biodegradable characteristics is treated by coagulation, flocculation, heterogeneous photocatalyst and membrane filtration techniques (Alexander et al. 2012; Barahimi et al. 2019; Ong et al. 2014). Rafiee et al. reported that the dye removal from LEP wastewater is achieved about 90% at COD concentration of 350 mg/L by polyoxometalate-TiO_2 nanocomposite (Rafiee et al. 2020).

The water pollution from heavy metal ions has been known as another serious challenge. Despite the necessity of some heavy metals as copper, selenium and zinc for living organisms, they can be considered as harmful trace elements when taken at concentrations over permissive limit. For instance, the presence of the excess amounts of copper ions (Cu^{+2}) in the human body might be responsible for strong health problems. Thus, they must be effectively eliminated from polluted effluents before introducing into water systems. Accordingly, various techniques are applied to remove heavy metal ions like solvent extraction, adsorption, precipitation, membrane filtration and ion exchange (Fang et al. 2018; Huang et al. 2018; Martín et al. 2018; Zare et al. 2018). Generally, the adsorption process is being grown interested in wastewater treatment to remove heavy metals and dyes because of its excellent benefits (Ahluwalia and Goyal 2007). The extensive researches have already been focused on a series of porous materials such as natural inorganic, polymers and metallic nanoparticles as absorbance agents. Among these studies, the utilization of metal oxide nanoparticles as a nano-adsorbent has been getting a hot research issue (Ghorbannezhad et al. 2018; Hua et al. 2012). However, the separation and regeneration of nano-adsorbents from treated water have restricted their application.

On the other hand, nanoparticles tend to be agglomerated during adsorption process due to having high interfacial energy. Consequently, adsorption ability decreases during passing time (Gupta and Gupta 2005). In order to overcome these challenges, the best way is embedding these nano-adsorbents into membrane matrix as porous support and preparation of nanocomposite membrane. However, it should be noted membrane fouling is the biggest obstacle for membranes, hampering their widespread application (Burman and Sinha 2018; Saljoughi et al. 2013; Won et al. 2012). So, incorporating nano-adsorbents into membrane body itself is an effective method to the mitigation of fouling phenomena (Yang and Mi 2013), since these adsorptive membranes possess different hydrophilic functional groups on the external and internal surfaces like –COOH, –SO_3H or –NH_2 which can bond with heavy metal ions and also promote membrane hydrophilicity (Dereli et al. 2012; Saljoughi et al. 2013; Won et al. 2012). During recent years, many studies have been dedicated to blending metal oxide nanoparticles into membrane casting solution, like Fe_3O_4 (Ghaemi 2016b; Rahimi et al. 2014), Al_2O_3 (Maximous et al. 2010), ZnO (Dipheko et al. 2017), TiO_2 (Das 2014), graphene oxide (GO) (Safarpour et al. 2016) and ZrO_2 (Pang et al. 2014) to impart high hydrophilicity, fouling resistance and water flux to membranes. Among those, titanium dioxide (TiO_2) nanoparticle with adsorptive properties has gained too much attention in membrane fabrication owing to its prominent advantages (Safarpour et al. 2015; Yang et al. 2006). However, the interfacial interaction between polymeric matrix and inorganic nanoparticles is weak, which limits their application in the membrane preparation. Therefore, the surface of inorganic nanoparticles is modified with different organic agents to form functional desire groups on its surface (Ghaemi and Daraei 2016; Jin et al. 2019).

The present study is an attempt to prepare polyethersulphone (PES) nanofiltration (NF) membranes modified with a novel kind of nanoparticles, which simultaneously enhance photocatalytic and filtration properties of membranes. The TiO_2-based nanoparticles are synthesized and functionalized with metformin with the help of silane coupling agent 3-cyanopropyltriethoxysilane (CPTES). The available data in the literature reflected that no study has been reported to synthesis adsorptive membranes modified with metformin-functionalized TiO_2 and its application to eliminate Cu^{+2} ions from aqueous solution and organism pollutants from liquorice extraction plant wastewater. In this work, the effect of this new type of additive was examined on adsorptive and antifouling characteristics of the prepared membranes. SEM, AFM and water contact angle measurements have been studied to the characterization of membranes.

Experimental

Materials

Metformin hydrochloride (*N*,*N*-dimethylbiguanide), 3-cyanopropyltriethoxysilane (CPTES) and Poly (*N*-vinylpyrrolidone) (PVP, $M_w = 29{,}000$) were purchased from Sigma-Alderich, UK. Tetraisopropyltitanate ($C_{12}H_{28}O_4Ti$, TIPT, 99 wt%), Copper(II) nitrate ($Cu(NO_3)_2$), *N*,*N*-dimethyl acetamide (DMAc), acetonitrile, toluene, ethanol (99.9 wt%), hydrochloric acid (HCl), potassium carbonate (K_2CO_3) and potassium iodide (KI) were purchased from Merck, Germany. Polyethersulfone (PES, $M_w = 58{,}000$ g mol^{-1}, Ultrason E6020P) was obtained from BASF, Germany. Liquorice wastewater was collected from Zagros liquorice company, Kermanshah, Iran.

Fabrication of metformin-functionalized TiO_2 with silane coupling agent

TiO_2 nanoparticles

TIPT (12 ml) was dropped into the mixture of ethanol (33 ml) and HCl (1 ml, 12 M) under vagarious stirring. The final solution was aged for 24 h at room temperature and then dried at 80 °C for 12 h. The dried powder was calcined at 450 °C for 2.5 h.

TiO_2/CPTES/metformin nanocomposites

The synthesized TiO_2 nanoparticles (0.5 g) were dispersed in 0.5 ml of CPTES (0.5 ml) solution and dissolved in 50 ml of toluene. The solution was kept under ultrasonic bath (1 h) and then was refluxed (24 h at 110 °C) to generate activated SiO_2-Cl groups on the edges of TiO_2 particles. The TiO_2/CPTES/metformin hybrid was synthesized from 0.5 g TiO_2/CPTES and dispersed in 30 ml acetonitrile and 0.15 g metformin, 0.6 g K_2CO_3, and 0.8 g KI was added and stirred for 24 h at 80 °C. The white mixture was filtered and washed copiously with deionized water and ethanol and then dried in a vacuum at 70 °C. Eventually, the resulted magnetic product is TiO_2/CPTES/metformin hybrid.

Fabrication of PES-TiO_2/CPTES/metformin NF membrane

The NF membranes were prepared using the phase inversion method. The desired amount of TiO_2/CPTES/metformin NPs (0, 0.1, 0.5 and 1 wt% corresponding to M_0, M_1, M_2 and M_3, respectively) were dispersed in solvent (DMAc) under ultrasonic bath and then pore former (PVP, 1 wt%), and polymer (PES, 20 wt%) was added to the casting solution under stirring for 24 h. To remove air bubbles, the casting solution was kept at ultrasonic bath and casted on a glass substrate using a homemade film applicator with 200 µm thickness. After casting step, the casted membrane film on the glass plate is placed on the coagulation bath with water as a non-solvent. Then, the membrane is maintained in distilled water (24 h and 25 °C). Finally, the membranes were sandwiched between two sheets of filter paper and let them be dried at room temperature for 24 h.

Characterization method

Crystal structure of the TiO_2/CPTES/metformin nanoparticles was determined using Rigaku D-max C III, X-ray diffractometer with CuKa emission at room temperature. The functional group of nanostructure was also investigated using FT-IR spectrometer (Shimadzu Varian 4300).

The morphological information of the prepared nanoparticles and membranes was assessed by scanning electron microscopy (SEM, Philips XL 30 and S-4160). Before the cross-sectional morphology images were taken, the membrane samples were fractured in liquid nitrogen and then sputtered with Au. The membrane surface morphology and roughness significantly influence the membrane properties, because the first place of the membrane subjecting to feed solution is the membrane surface. Therefore, separation performance of membrane is affected by the surface morphology. The roughness surface morphology was analyzed using atomic force microscopy (AFM) images (DMFASTSCAN-SYS, Bruker, Germany). In order to determine the membrane hydrophilicity, the sessile drop method (contact angle goniometer, OCA20, Dataphysics Instrument, Germany) was used to measure static water contact angle. To minimize the experimental error, an average value of at least four or five random points on each membrane surface was reported as water contact angle.

Permeability and antifouling measurements

A batch-type stainless steel dead-end setup (volume of 125 ml and 12.56 cm^2 of effective membrane surface area) equipped with a nitrogen gas capsule was used to evaluate membrane performance (Fig. 1). The feed solution was stirred at the rate of 400 rpm to remove the polarization concentration effect. It is noted that at least five replicates have been carried out for each test to diminish the experimental error.

First, each membrane (with an effective area of 12.56 cm^2) was pre-compacted at 4 bar with DI water for 30 min to attain a stable flux. The permeate flux, $J_{w,1}$ (kg m^{-2} h^{-1}), was determined by Eq. 1 as given below:

$$J = \frac{Q}{A \cdot \Delta t} \quad (1)$$

where A, Δt and Q are the effective membrane area (m^2), time (h) and permeate weight (kg), respectively.

Milk powder-suspended solution as good fouling agent is used to study the fouling process in detail, and fouling resistance parameters were calculated to investigate the fouling resistant ability of the prepared membrane (Zangeneh et al. 2019). In general, fouling takes places owing to the development of a cake or gel layer on the membrane surface and/

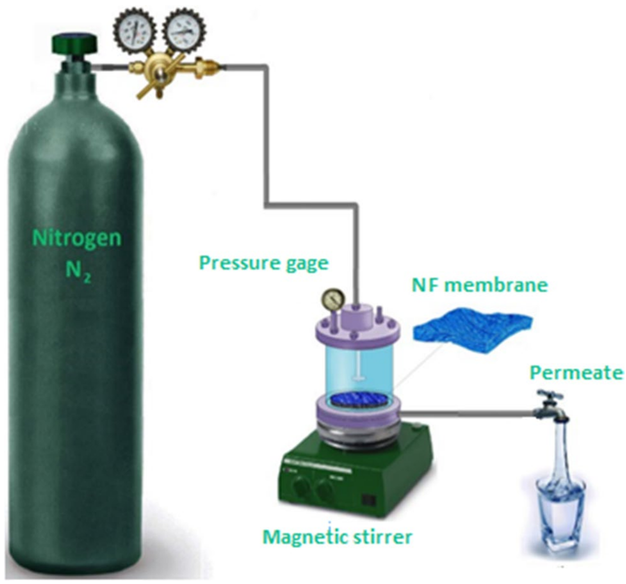

Fig. 1 Schematic flow diagram of the dead-end experimental cell

or adsorption onto the surface or inside of the membrane pores. Irreversible fouling (R_{ir}) indicates the fouling which is caused by stable connection of foulants on the membrane surface; meanwhile, reversible fouling (R_r) defines the fouling resulted from concentration polarization. Therefore, the minor irreversible fouling is because of an effective antifouling ability of the membrane.

For antifouling test, after first pure water flux, the filtration cell was rapidly refilled with the milk powder-suspended solution (8000 mg l^{-1}) and its water flux (J_p) is measured again for 90 min. Afterward, distilled water is used to clean and wash the fouled membrane (30 min). Then, the pure water flux was determined again and notated as $J_{w,2}$ (kg m^{-2} h^{-1}). The fouling resistance and flux recovery ratio (FRR) were calculated as follows (Jin et al. 2019):

$$R_t(\%) = \left(1 - \frac{J_p}{J_{w,1}}\right) \times 100 \quad (2)$$

$$R_r(\%) = \left(\frac{J_{w,2} - J_p}{J_{w,1}}\right) \times 1 \quad (3)$$

$$R_{ir}(\%) = R_t - R_r \quad (4)$$

$$\text{FRR}\ (\%) = \frac{J_{w,2}}{J_{w,1}} \times 100 \quad (5)$$

Copper removal experiments

The aqueous solution of $Cu(NO_3)_2$ (20 mg l^{-1}) with pH of 5.0 was used to evaluate the ability of the prepared membrane for copper rejection. Since $Cu(OH)_2$ is precipitated at pH higher than 6, all the experiments were performed at pH of 5.0 and ambient temperature in dead-end filtration cell (Fig. 1). The copper removal efficiency was calculated as given below equation (Abdi et al. 2018):

$$\text{Copper removal}(\%) = \left(1 - \frac{C_p}{C_f}\right) \times 100 \quad (6)$$

where C_p and C_f are the concentration of the copper ion in the permeated and feed solutions (mg l^{-1}), respectively. The Cu^{+2} content was determined using an atomic adsorption spectrophotometer (210VGP model, Buck company, USA, with copper hollow cathode lamp).

In reusability test, the membrane is dipped in EDTA solution (10 mM and pH of 10.5) about 1 h and washed with deionized water and repeated test for four cycles.

LEP wastewater treatment

The filtration of LEP wastewater is also investigated at pressure of 5 bar for 120 min. Characteristics LEP wastewater is shown in Table 1. The COD and dye removals were calculated using the following equations:

$$\text{COD removal}(\%) = \left(\frac{\text{COD}_f - \text{COD}_p}{\text{COD}_f}\right) \times 100 \quad (7)$$

$$\text{Dye removal}(\%) = \left(\frac{A_f - A_p}{A_f}\right) \times 100 \quad (8)$$

where COD_f or A_f and COD_p or A_p are the COD concentration or average absorption of the feed and the permeate solution, respectively.

Table 1 Characteristics of biologically of liquorice wastewater

Wastewater properties	Initial conditions before treatment
Color	Brown
COD	700–800
BOD_5/COD ratio	0.17–0.19
pH	5.7–6.4
TSS	120

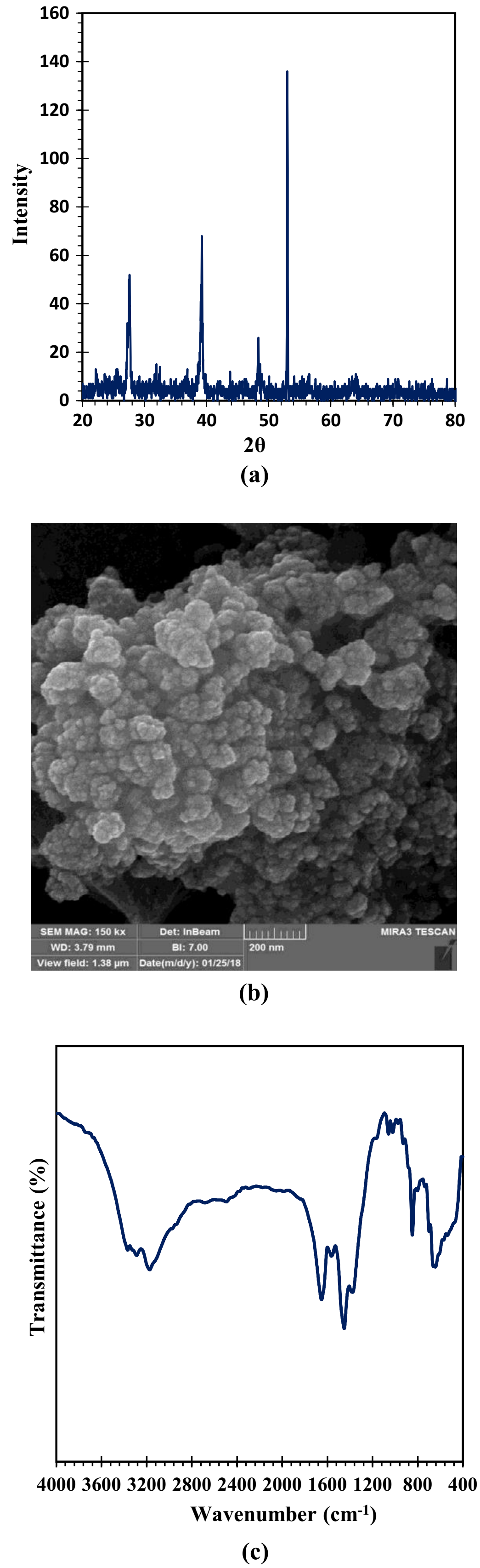

Fig. 2 **a** XRD pattern and **b** SEM image and **c** FT-IR spectrum of ▶ TiO_2/CPTES/metformin nanocomposite

Results and discussion

Characterization of TiO_2/CPTES/metformin nanoparticles

The properties of prepared TiO_2/CPTES/metformin nanoparticles are shown in Fig. 2a–c. The anatase TiO_2 was completely confirmed with occurrence of the observed XRD reflection peaks (JCPDS cards 21-1272 and 21-1276) which are appeared at 2θ of 27.3°, 39.2°, 48.3°, 53.0°, 63.4° (Fig. 2a).

Figure 2b shows the SEM image of the TiO_2/CPTES/metformin nanocomposite. It was observed that the sample is composed of spherical nanoparticles which their average particle size is 36 nm.

In FT-IR spectrum of TiO_2/CPTES/metformin nanocomposite (Fig. 2c), the wide absorbance peak at 743.04 and 799.53 cm^{-1} is corresponding to the Ti–O and Ti–O–Ti vibration bonds (Hamadanian et al. 2016). The peak in 1021.02 cm^{-1} is antisymmetric stretching vibration of Si–O–Si. The C=N and C–N stretching vibration of primary amine in metformin are appeared at 1584.12 and 1059.18 cm^{-1}, respectively, which confirmed formation of metformin external shell over NPs. The peaks at 1630–1651 and 3173.53–3369.04 cm^{-1} are assigned to O–H and N–H stretching and bending vibrations, respectively (Wei et al. 2014). The water contact angles for the blend nanocomposites membranes (Fig. 3) are agreed with the moisture peaks of FT-IR of TiO_2/CPTES/metformin nanocomposite.

Characterization of the PES-TiO_2/CPTES/metformin nanocomposite membranes

The membrane hydrophilicity is evaluated using the water contact angels measurement as shown in Fig. 3a. The water contact angle and pure water flux of the unfilled PES and PES-TiO_2/CPTES/metformin nanocomposite membranes are shown in Fig. 3a, b, respectively. The water contact angles were reduced with the addition of the nanoparticles. The water contact angle values of M_0, M_1, M_2 and M_3 membranes are 64°, 58°, 52° and 50.2°, respectively. This result has established that the hydrophilic nature of the contributed nanoparticles into membrane matrix led to improve the affinity of water to wet the membrane surface, thereby increasing membrane hydrophilicity (Soloukipour et al. 2017). It was demonstrated that the spontaneous movement of hydrophilic nanofillers to the membrane/water interface in the coagulation bath has resulted in the improvement in membrane hydrophilicity. Therefore, the

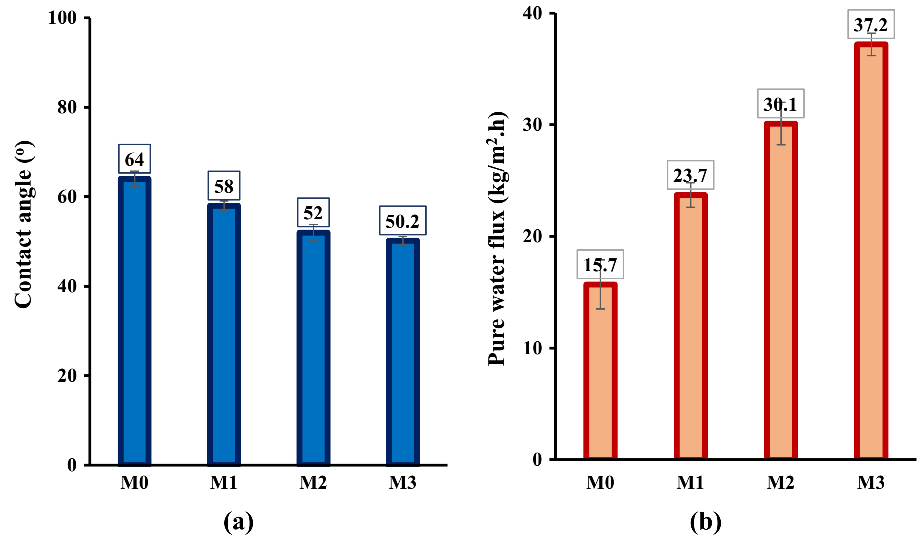

Fig. 3 **a** Water contact angle and **b** pure water flux of the prepared membranes

presence of hydroxyl and amino groups on the membrane surface corresponds to increase membrane hydrophilicity (Bojaran et al. 2019). Similar observations were also reported in a study of Vadanpour and his coworkers (Vatanpour et al. 2012).

As observed in Fig. 3b, the pure water flux of the fabricated membranes increases with incorporation of TiO_2/CPTES/metformin NPs in PES matrix. It is documented the enhancement in membrane hydrophilicity as shown in Fig. 2a. Also, the increase in membrane porosity (SEM images, Fig. 4) leads to the increment in membrane permeability (Ghaemi 2016b; Zangeneh et al. 2018). It is noted that 1% of NPs (M_3) nanocomposite membrane has the best permeability compared to other the prepared membranes.

The cross-sectional SEM images of M_0, M_1, M_2 and M_3 membranes are displayed in Fig. 4a–h, respectively. The asymmetric structure with two layers including a dense skin and soft finger structure in sub-layers was observed for all membranes. With the addition of TiO_2/CPTES/metformin nanocomposites to PES matrix, the number of finger-like porous in the sub-layer increased and spongy structure with bulk-size porous appeared. The fast exchange between water and DMAc in coagulation bath was occurred due to the introduction of hydrophilic TiO_2/CPTES/metformin nanoparticles which is improved membrane hydrophilicity and expanded the population of pores (Razmjou et al. 2012; Zeng et al. 2016).

The AFM topology investigation for M_0, M_1, M_2 and M_3 membranes are displayed in Fig. 5. The modified membranes had a significant change after adding hydrophilic nanoparticles in comparison with the bare membrane. Those modified membranes presented fewer peaks and valleys than those of the bare membrane. It is attributed to moving the hydrophilic nanoparticles to the membrane surface, which fill the membrane surface valleys during the membrane solidification. It ought to be noted that in the wastewater treatment process, a rough surface is willing to be filled by existence pollutants, which cannot be removed easily through water or other reagents. Therefore, the reduction in the flux and rejection will be its consequence (Zangeneh et al. 2018).

Membrane performance

Antifouling test

Figure 6 illustrates the FRR values for M_0, M_1, M_2, and M_3 membranes. It can be seen that PES-TiO_2/CPTES/metformin membranes show relatively better antifouling properties than the unfilled PES membrane. The enhancement of antifouling performance of the blended membranes is due to the improvement in hydrophilic properties of modified membranes (Fig. 3) and reduction in the membrane roughness with the addition of NPs (Zangeneh et al. 2019; Zinadini et al. 2014). The R_r/R_t and R_{ir}/R_t ratios were also calculated as shown in Table 2. The result indicated that R_{ir}/R_t ratio for modified membranes diminishes compared to the unfilled PES membrane, while R_r/R_t ratio is increased with the addition of NPs into PES matrix. It is due to decrease in the deposition and entrapment of fouling agent on the membrane surface or pores (Zangeneh et al. 2019).

Cu(II) rejection

Figure 7 shows Cu(II) rejection of unfilled PES and nanocomposite membranes. The values of Cu(II) rejections are for 26.7, 67.3, 77.1 and 90.1 for M_0, M_1, M_2 and M_3 membranes. The improvement in membrane performance for Cu

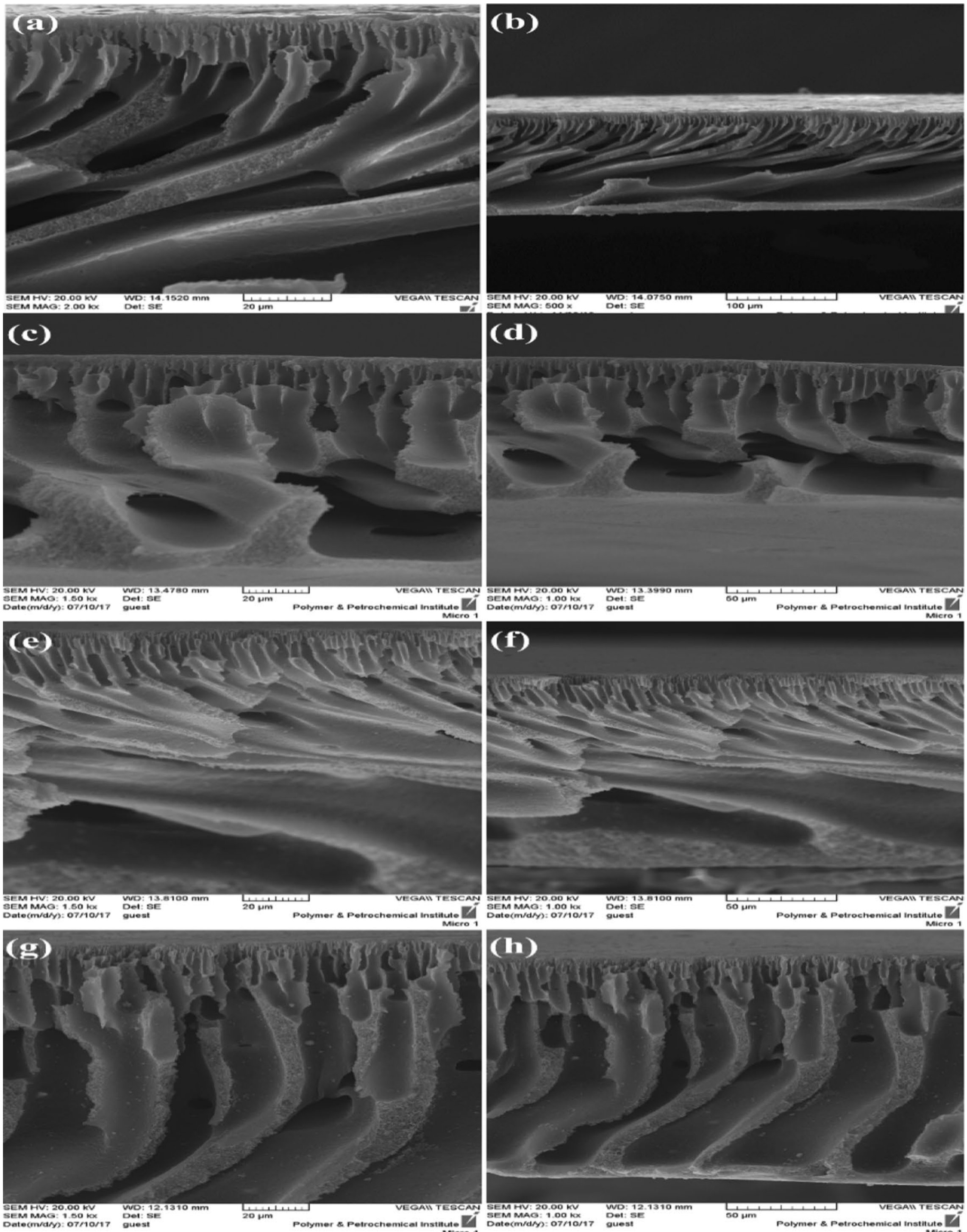

Fig. 4 SEM images of **a**–**b** M_0, **c**–**d** M_1, **e**–**f** M_2 and **g**–**h** M_3 membranes

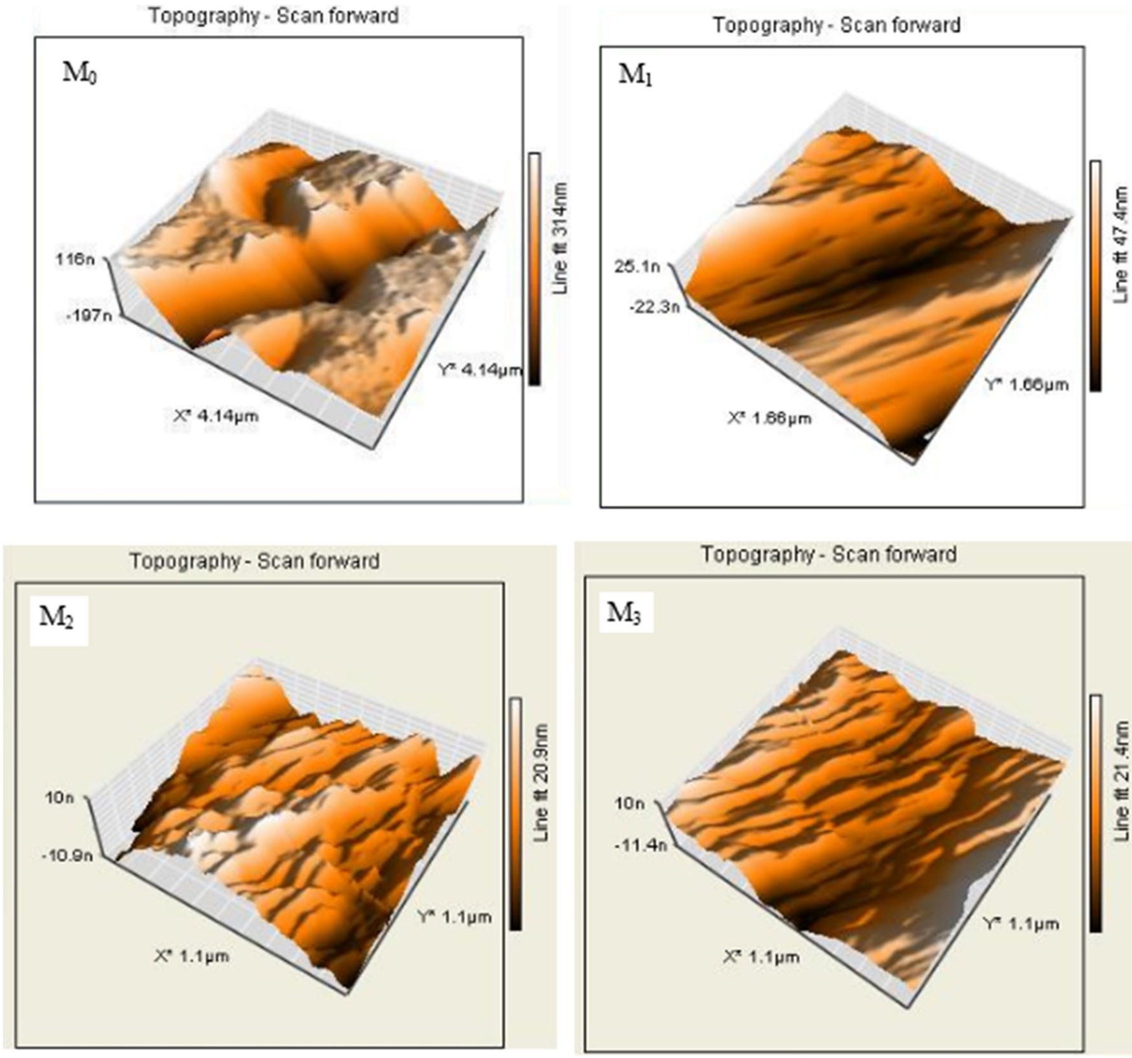

Fig. 5 AFM surface images of the prepared membranes

removal is due to the interaction between nitrogen atoms with lone electron pairs in amine group on the membrane surface and Cu(II) ions. Also, a higher dispersion of NPs as hydrophilic species on the membrane surface cause to increase the available adsorption sites on the membrane surface, thereby improving Cu rejection for modified membranes.

The M_3 nanocomposites membrane (1% of NPs) was selected to study its reusability performance for four cycles (Fig. 8). No significant decrease in membrane rejection was observed during the recycling study. The results mean that the nature and stability of active nitrogen sites did not change on M_3 nanocomposites membrane after being used repetitively for four times.

LEP wastewater treatment

Figure 9 displays the rejection and permeate flux of all membranes during filtration of LEP wastewater with COD concentration of 800 mg l^{-1} at pressure of 5 bar after 150 min. The modified membranes indicate high permeate flux (M_1, M_2 and M_3, for 79.1, 82.7 and 88 kg m^{-2} h^{-1}) compared to the unfilled PES membrane (M_0, 74.5 kg m^{-2} h^{-1}). The high permeate flux of the modified membranes compared to unfilled PES membrane is due to the hydrophilicity and ultrafine (special morphology and topography) properties of the blended PES membranes. The value of permeate flux was higher for M_3 membranes. However, the dye and COD removal efficiencies for the unfilled PES membrane and blended membranes were not obviously changed

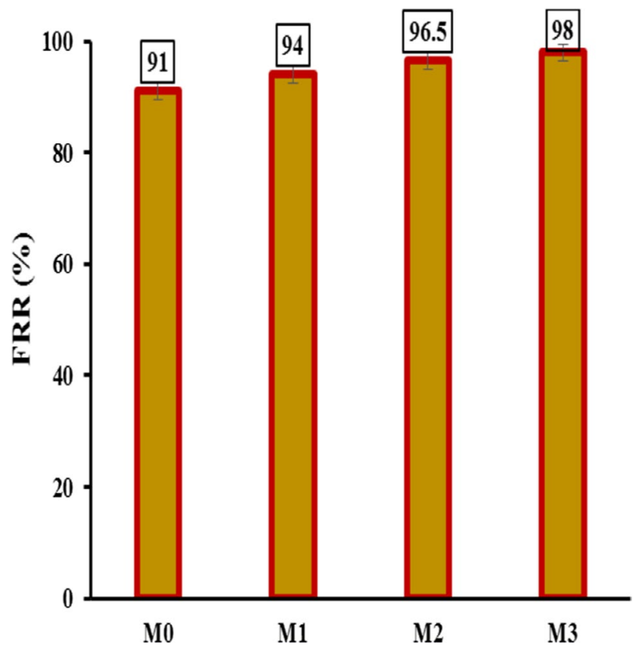

Fig. 6 FRR values of the prepared membranes during filtration of milk powder with concentration of 8000 mg l^{-1}

Table 2 Fouling parameters of the prepared membranes

Membrane types	R_r/R_t	R_{ir}/R_t
M_0	0.17	0.83
M_1	0.61	0.39
M_2	0.67	0.33
M_3	0.73	0.27

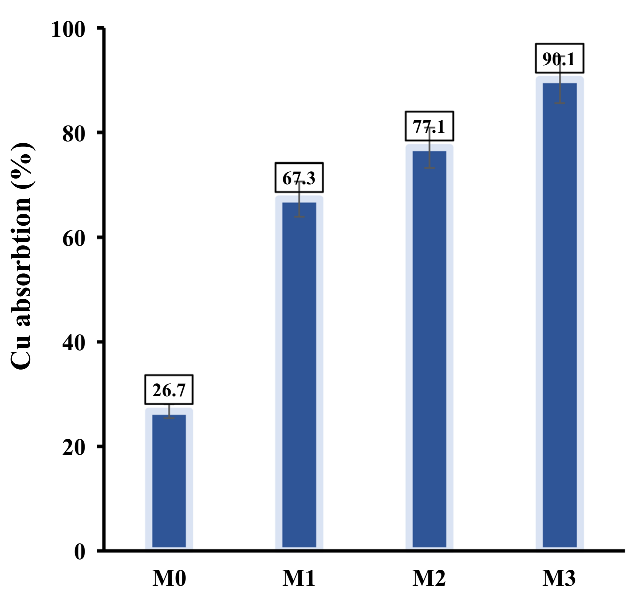

Fig. 7 Cu(II) rejection of the prepared membranes for 20 ppm $Cu(NO_3)_2$ solution in the pH of 5 after 60 min

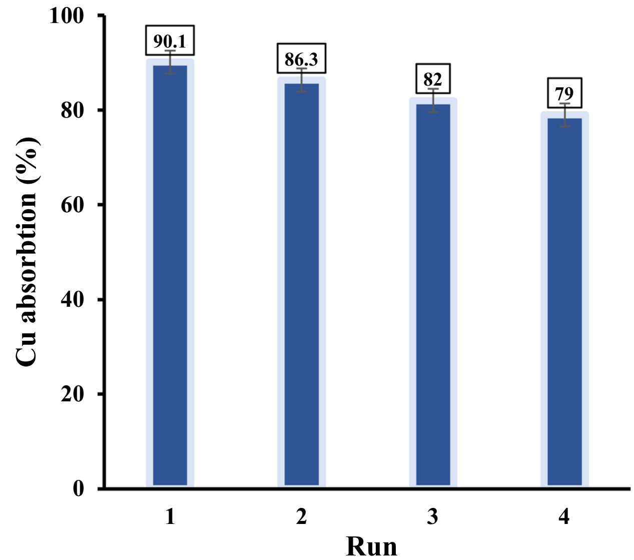

Fig. 8 Reusability of M_3 nanocomposites membrane (M_3) in Cu(II) rejection test for 20 ppm $Cu(NO_3)_2$ solution in the pH of 5

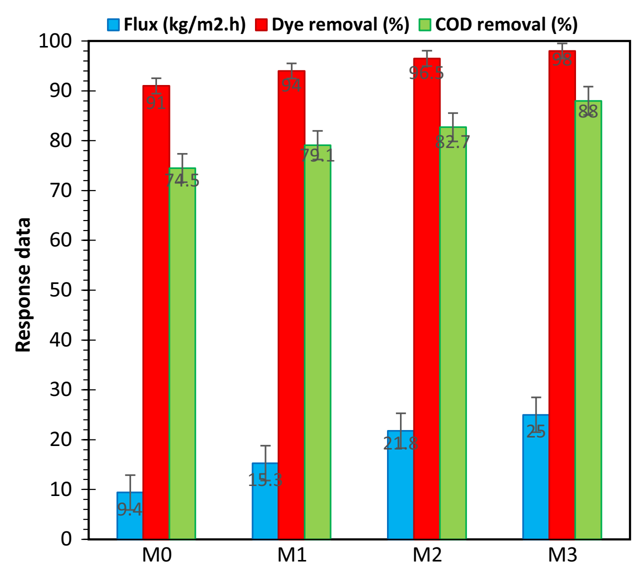

Fig. 9 Performance of the prepared membranes in treatment of the LEP wastewater with initial COD concentration of 800 mg l^{-1} at 5 bar after 150 min

(91, 94, 96.5 and 98% for M_0, M_1, M_2 and M_3 membranes, respectively).

Long-term performances of M_3 membrane

Other examination for testing antifouling properties of the membrane was to measure the permeation flux decline during a long period for the LEP wastewater. The unfilled PES membrane (M_0) and optimally modified membrane (M_3)

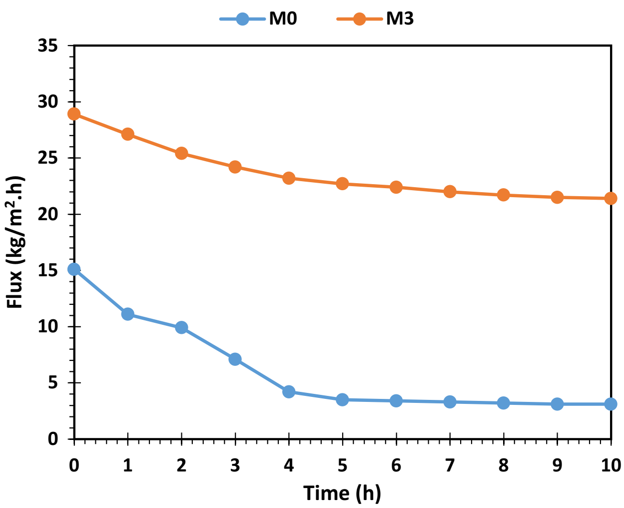

Fig. 10 Flux decline of M_0 and M_3 membranes during 10 h filtration of the LEP wastewater for initial COD of 700 mg l^{-1} at 5 bar after 10 h

were chosen to measure the permeation flux during filtration of the LEP wastewater as shown in Fig. 10.

The trend of M_0 and M_3 permeate flux shows a decrease during LEP wastewater filtration. The adsorption or deposition of organic content with various molecular weight in the LEP wastewater on the membrane surface or pores increases the membrane fouling, so permeation flux is reduced (Zangeneh et al. 2020). The fouling of the M_0 membrane becomes stable sooner than that of the M_3 membrane. It means that pore blocking occurs faster in the M_0 membrane compared to M_3 modified membrane.

The performance of M_3 nanocomposite membrane in terms of Cu rejection and COD removal from LEP wastewater was also compared with another published modified NF membranes for rejection Cu ions and organic pollutants as represented in Table 3. In the present study, the Cu rejection, COD removal and dye removals from LEP wastewater were achieved about for M_3 membrane which is approved a good performance of TiO_2/CPTES/Metformin/PES nanocomposite membrane.

Conclusion

The overall aim of this study is to synthesize and characterize a novel antifouling PES nanocomposite membrane. The performance of TiO_2/CPTES/Metformin/PES nanocomposites membranes was successfully evaluated in terms of pure water flux, Cu(II) ion rejection from aqueous solution and COD or dye removal from LEP wastewater. The maximum values of pure water flux, FRR, Cu rejection, COD and dye removal from LEP wastewater were achieved at 1% of NPs. The antifouling result indicated that the membrane fouling reduces with the adding of NPs due to increase membrane hydrophilicity and reduce its roughness which are approved by contact angle and AFM analysis, respectively. The blended PES membranes showed excellent performance for rejections of Cu ions from aqueous solution and COD or dye removals from LEP wastewater.

Table 3 Comparison the performance of NF membranes between TiO_2/CPTES/Metformin/PES nanocomposite membrane and previous studies

Type of NF membrane	Pollutant	Rejection	Operating conditions	References
Magnetic graphene oxide/metformin/PES	Cu ions	98% after 100 min	[Cu $(NO_3)_2$] = 20 mg l^{-1} Pressure = 4 bar	Abdi et al. (2018)
	Direct red 16	99% after 60 min	[Dye] = 30 mg l^{-1} Pressure = 4 bar	
Polypyrrole @ Al_2O_3/PES	Cu ions	81% after 110 min	[Cu $(NO_3)_2$] = 20 mg l^{-1} Pressure = 4 bar	Ghaemi and Daraei (2016)
Al_2O_3/PES	Cu ions	81% after 110 min	[Cu $(NO_3)_2$] = 20 mg l^{-1} Pressure = 4 bar	Ghaemi (2016b)
Fe_3O_4/PES	Cu ions	35% after 90 min	[Cu $(NO_3)_2$] = 20 mg l^{-1} Pressure = 4 bar	Ghaemi (2016a)
Fe_3O_4/SiO_2/PES		49% after 90 min		
Fe_3O_4/SiO_2/metformin/PES		94% after 90 min		
Fe_3O_4/SiO_2APTES/PES		82% after 90 min		
TiO_2/CPTES/metformin/PES	Cu ions	90.1% after 60 min	[Cu $(NO_3)_2$] = 20 mg l^{-1} Pressure = 4 bar	This work
TiO_2/CPTES/metformin/PES	LEP wastewater	COD removal = 88% after 150 min	[COD] = 800 mg l^{-1} Pressure = 4 bar	

References

Abdi G, Alizadeh A, Zinadini S, Moradi G (2018) Removal of dye and heavy metal ion using a novel synthetic polyethersulfone nanofiltration membrane modified by magnetic graphene oxide/metformin hybrid. J Membr Sci 552:326–335

Ahluwalia SS, Goyal D (2007) Microbial and plant derived biomass for removal of heavy metals from wastewater. Bioresour Technol 98:2243–2257

Alexander JT, Hai FI, Al-aboud TM (2012) Chemical coagulation-based processes for trace organic contaminant removal: current state and future potential. J Environ Manag 111:195–207

Barahimi V, Moghimi H, Taheri RA (2019) Cu doped TiO_2-Bi_2O_3 nanocomposite for degradation of azo dye in aqueous solution: process modeling and optimization using central composite design. J Environ Chem Eng 7:103078

Bojaran M, Akbari A, Yunessnia Lehi A (2019) Novel ultrafiltration membranes with the least fouling properties for the treatment of veterinary antibiotics in the pharmaceutical wastewater. Polym Adv Technol 30:1716–1723

Burman I, Sinha A (2018) A review on membrane fouling in membrane bioreactors: control and mitigation. In: Environmental contaminants. Springer, Berlin, pp 281–315

Das R (2014) Application photocatalysis for treatment of industrial waste water—a short review. Open Access Libr J 1:1

Dereli RK, Ersahin ME, Ozgun H, Ozturk I, Jeison D, van der Zee F, van Lier JB (2012) Potentials of anaerobic membrane bioreactors to overcome treatment limitations induced by industrial wastewaters. Bioresour Technol 122:160–170

Dipheko TD, Matabola KP, Kotlhao K, Moutloali RM, Klink M (2017) Fabrication and assessment of ZnO modified polyethersulfone membranes for fouling reduction of bovine serum albumin. Int J Polym Sci 2017:1–8

Fang L, Li L, Qu Z, Xu H, Xu J, Yan N (2018) A novel method for the sequential removal and separation of multiple heavy metals from wastewater. J Hazard Mater 342:617–624

Ghaemi N, Daraei P (2016) Enhancement in copper ion removal by PPy@ Al_2O_3 polymeric nanocomposite membrane. J Ind Eng Chem 40:26–33

Ghaemi N (2016a) A new approach to copper ion removal from water by polymeric nanocomposite membrane embedded with γ-alumina nanoparticles. Appl Surf Sci 364:221–228

Ghaemi N (2016b) Polyethersulfone membrane enhanced with iron oxide nanoparticles for copper removal from water: application of new functionalized Fe_3O_4 nanoparticles. Chem Eng J 263:101–112

Ghorbannezhad H, Moghimi H, Taheri RA (2018) Enhanced biodegradation of phenol by magnetically immobilized trichosporon cutaneum. Ann Microbiol 68:485–491

Gupta AK, Gupta M (2005) Synthesis and surface engineering of iron oxide nanoparticles for biomedical applications. Biomaterials 26:3995–4021

Hamadanian M, Karimzadeh S, Jabbari V, Villagrán D (2016) Synthesis of cysteine, cobalt and copper-doped TiO_2 nanophotocatalysts with excellent visible-light-induced photocatalytic activity. Mater Sci Semicond Process 41:168–176

Hua M, Zhang S, Pan B, Zhang W, Lv L, Zhang Q (2012) Heavy metal removal from water/wastewater by nanosized metal oxides: a review. J Hazard Mater 211:317–331

Huang Y, Zeng X, Guo L, Lan J, Zhang L, Cao D (2018) Heavy metal ion removal of wastewater by zeolite-imidazolate frameworks. Sep Purif Technol 194:462–469

Jin Y, Hu D, Yk Lin, Shi L (2019) Hydrophilic modification of polyvinylidene fluoride membrane by blending amphiphilic copolymer via thermally induced phase separation. Polym Adv Technol 30:110–119

Martín DM, Faccini M, García M, Amantia D (2018) Highly efficient removal of heavy metal ions from polluted water using ion-selective polyacrylonitrile nanofibers. J Environ Chem Eng 6:236–245

Maximous N, Nakhla G, Wong K, Wan W (2010) Optimization of Al_2O_3/PES membranes for wastewater filtration. Sep Purif Technol 73:294–301

Ong YK, Li FY, Sun S-P, Zhao B-W, Liang C-Z, Chung T-S (2014) Nanofiltration hollow fiber membranes for textile wastewater treatment: lab-scale and pilot-scale studies. Chem Eng Sci 114:51–57

Pang R, Li X, Li J, Lu Z, Sun X, Wang L (2014) Preparation and characterization of ZrO_2/PES hybrid ultrafiltration membrane with uniform ZrO_2 nanoparticles. Desalination 332:60–66

Rafiee E, Pami N, Zinatizadeh AA, Eavani S (2020) A new polyoxometalate-TiO_2 nanocomposite for efficient visible photodegradation of dye from wastewater, liquorice and yeast extract: photoelectrochemical, electrochemical, and physical investigations. J Photochem Photobiol A Chem 386:112145

Rahimi Z, Zinatizadeh AA, Zinadini S (2014) Preparation and characterization of a high antibiofouling ultrafiltration PES membrane using OCMCS-Fe3O4 for application in MBR treating wastewater. J Appl Res Water Wastewater 1:13–17

Razmjou A, Arifin E, Dong G, Mansouri J, Chen V (2012) Superhydrophobic modification of TiO_2 nanocomposite PVDF membranes for applications in membrane distillation. J Membr Sci 415:850–863

Safarpour M, Khataee A, Vatanpour V (2015) Effect of reduced graphene oxide/TiO_2 nanocomposite with different molar ratios on the performance of PVDF ultrafiltration membranes. Sep Purif Technol 140:32–42

Safarpour M, Vatanpour V, Khataee A (2016) Preparation and characterization of graphene oxide/TiO_2 blended PES nanofiltration membrane with improved antifouling and separation performance. Desalination 393:65–78

Saljoughi E, Mousavi SM, Hosseini SA (2013) Polysulfone/Brij-58 blend nanofiltration membranes: preparation, morphology and performance. Polym Adv Technol 24:383–390

Soloukipour S, Saljoughi E, Mousavi SM, Pourafshari Chenar M (2017) PEBA/PVDF blend pervaporation membranes: preparation and performance. Polym Adv Technol 28:113–123

Vatanpour V, Madaeni SS, Khataee AR, Salehi E, Zinadini S, Monfared HA (2012) TiO_2 embedded mixed matrix PES nanocomposite membranes: influence of different sizes and types of nanoparticles on antifouling and performance. Desalination 292:19–29

Wei X, Wang S, Shi Y, Xiang H, Chen J (2014) Application of positively charged composite hollow-fiber nanofiltration membranes for dye purification. Ind Eng Chem Res 53:14036–14045

Won Y-J, Lee J, Choi D-C, Chae HR, Kim I, Lee C-H, Kim I-C (2012) Preparation and application of patterned membranes for wastewater treatment. Environ Sci Technol 46:11021–11027

Yang Q, Mi B (2013) Nanomaterials for membrane fouling control: accomplishments and challenges. Adv Chronic Kidney Dis 20:536–555

Yang Y, Wang P, Zheng Q (2006) Preparation and properties of polysulfone/TiO_2 composite ultrafiltration membranes. J Polym Sci, Part B: Polym Phys 44:879–887

Zangeneh H, Zinatizadeh AA, Zinadini S, Feyzi M, Bahnemann DW (2018) A novel photocatalytic self-cleaning PES nanofiltration membrane incorporating triple metal-nonmetal doped TiO_2 (KBN-TiO2) for post treatment of biologically treated palm oil mill effluent. React Funct Polym 127:139–152

Zangeneh H, Zinatizadeh AA, Zinadini S, Feyzi M, Bahnemann DW (2019) Preparation and characterization of a novel photocatalytic self-cleaning PES nanofiltration membrane by embedding a visible-driven photocatalyst boron doped-TiO_2SiO_2/$CoFe_2O_4$ nanoparticles. Sep Purif Technol 209:764–775

Zangeneh H, Zinatizadeh AA, Zinadini S (2020) Self-cleaning properties of L-Histidine doped TiO2-CdS/PES nanocomposite membrane: fabrication, characterization and performance. Sep Purifi Technol 240:116591

Zare EN, Motahari A, Sillanpää M (2018) Nanoadsorbents based on conducting polymer nanocomposites with main focus on polyaniline and its derivatives for removal of heavy metal ions/dyes: a review. Environ Res 162:173–195

Zeng G, He Y, Zhan Y, Zhang L, Pan Y, Zhang C, Yu Z (2016) Novel polyvinylidene fluoride nanofiltration membrane blended with functionalized halloysite nanotubes for dye and heavy metal ions removal. J Hazard Mater 317:60–72

Zinadini S, Zinatizadeh AA, Rahimi M, Vatanpour V, Zangeneh H (2014) Preparation of a novel antifouling mixed matrix PES membrane by embedding graphene oxide nanoplates. J Membr Sci 453:292–301

Publisher's Note Springer Nature remains neutral with regard to jurisdictional claims in published maps and institutional affiliations.